Electrochemical Materials and Technologies

REVIEW

eISSN: 2949-0561

Cite this: Electrochem. Mater. Technol. 2 (2023) 20232018

Some aspects of hydrogen oxidation in solid oxide fuel cell: A brief historical overview

Denis Osinkin [a *]

Received: 21 August 2023
Accepted: 15 September 2023
Published online: 3 October 2023

DOI: 10.15826/elmattech.2023.2.018

Environmentally friendly and resource-efficient ways to generate, convert, store and transport electricity are important areas of scientific and technological development. Fuel cells are direct converters of chemical energy into electricity with low emissions of harmful components. One of the most promising types of fuel cells is the solid oxide fuel cell (SOFC). The electrical power generated by the SOFC is mainly limited by the ohmic resistance of the electrolyte and the polarization of the electrodes. The ohmic resistance can be reduced by reducing the thickness of the electrolyte. To reduce the polarization resistance, other approaches are needed, namely a detailed study of the mechanisms of electrode reactions and the determination of the nature of rate-determining stages. Until now, fuel oxidation at the anode of the SOFC, as opposed to oxygen reduction at the cathode, has not been well understood. Even for conventional nickel-ceramic anodes, there is no clear understanding of the nature of the rate-determining steps of hydrogen oxidation. This review provides a brief historical background on the development of SOFCs, some insights into the oxygen reduction mechanisms, and a more detailed review of the kinetics of hydrogen oxidation at SOFC anodes.

keywords: solid oxide fuel cell, kinetics, hydrogen, oxygen, electrode reaction, rate-determining step

© 2023, the Authors. This article is published in open access under the terms and conditions of the Creative Commons Attribution (CC BY) license http://creativecommons.org/licenses/by/4.0/).

1. Introduction

Solid oxides as components of electrochemical devices were first studied in the second half of the century before last. The first studies were performed on simple oxides (copper oxide, antimony oxide, etc.) and were not systematic. Schottky was the first researcher to formulate the requirements for a solid oxide to be used in electrochemical devices [1]. Later, the oxide mixture $ZrO_2 + Y_2O_3$ (CaO), the so-called Nernst mass [2, 3], obtained decades before Schottky's study, was found to satisfy these requirements. This set the direction for development of all modern electrochemical devices based on solid oxygen conducting electrolytes, and solid electrolytes based on ZrO_2 are still under active research. The first concepts of solid oxide fuel cells (SOFC) were proposed by Baur et al. in the first half of the last century [4, 5]. However, these works were not further developed because the authors did not adhere to any reasonable ideology in selecting materials for SOFCs. After the work of Carl Wagner, who showed the correlation between the conductivity of the solid electrolyte and the concentration of oxygen vacancies [6], more reasonable approaches to the selection of materials for SOFCs began to emerge. Since the 1960s, investigations in SOFC field has been actively developed in many countries. One of the pioneers in this direction can be considered Westinghouse Electric and the work of Weissbart and Ruka [7], who demonstrated a solid oxide fuel cell with an electrolyte based on doped zirconium oxide and platinum electrodes. The first studies on the kinetics and mechanisms of the electrode reactions of oxygen reduction and hydrogen oxidation have been carried out precisely on platinum electrodes of SOFC.

Typically, a SOFC consists of a gas-tight electrolyte

a: Kinetics laboratory, Institute of High-Temperature Electrochemistry, Yekaterinburg 620066, Russia

* Corresponding author: OsinkinDA@mail.ru

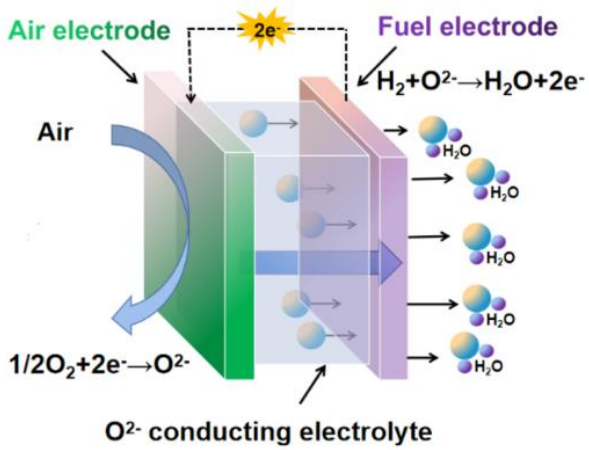

Figure 1 The sketch of a solid oxide fuel cell [8].

layer and two electrodes formed on opposite sides of the electrolyte (Figure 1). One of the electrodes (anode) is supplied with a fuel gas, such as hydrogen, and the other (cathode) is supplied with an oxidant containing molecular oxygen, which in most cases is air. At operating temperatures (500–900 °C), an EMF (electromotive force) of about one volt occurs between the SOFC electrodes. This is due to the difference in partial pressure of oxygen at the cathode and anode (Nernst law).

When no load is connected to the fuel cell (open circuit voltage mode), the rates of electrochemical reactions at the electrodes are close to equilibrium, i.e., the forward and reverse reaction rates are equal. When a load is connected to the fuel cell, oxygen is reduced at the cathode and hydrogen is oxidized at the anode. These electrochemical processes can be described in simplified terms as follows:

– reduction of molecular oxygen at the cathode to ions (Equation 1):

$$O_{2(gas)} + 4e^{-}{}_{(electrode)} = 2O^{2-}{}_{(electrolyte)} \quad (1)$$

– diffusion of oxygen ions through the solid electrolyte to the anode;

– the interaction of oxygen ions at the anode with hydrogen molecules with the formation of electrons and the hydrogen oxidation product, i.e. water (Equation 2):

$$H_{2(gas)} + O^{2-}{}_{(electrolyte)} = \\ = H_2O_{(gas)} + 2e^{-}{}_{(electrode)} \quad (2)$$

When the load is connected to the electrodes, an electric current begins to flow through it, resulting in a decrease in the potential difference between the electrodes U (Equation 3) relative to the open circuit EMF (E):

$$U = E - (I \cdot R_{\Omega}) - \eta_a - \eta_c, \quad (3)$$

where I – current, R_{Ω} – SOFC ohmic resistance, η_a and η_c – overvoltage of the anode and cathode, respectively.

There are two main reasons for the voltage drop; first, the SOFC has an ohmic resistance, which is mainly determined by the resistivity of the electrolyte (R_{Ω}); second, the electrochemical reactions at the cathode and anode do not occur instantaneously, but at a certain rate, which leads to current losses due to the polarization of the electrodes. Consequently, to increase the power generated by SOFCs, it is necessary to use electrolytes with high conductivity and electrodes with high electrochemical activity for the reactions of oxygen reduction and fuel oxidation.

To date, some of the most extensively studied oxide materials for use in oxygen electrodes are the complex oxides with the following general formula ABO_3, $A_2C_mD_{2-m}O_6$ and $A_{n+1}B_nO_{3n+1}$, where A – rare-earth or alkaline-earth element, B, C, D – usually 3 *d* element Cu, Ti, Cr, Mn, Fe, Co, Ni etc) [9–13].

In recent decades, the main material for fuel electrodes, i.e. SOFC anodes, has been a composite of metallic nickel and a ceramic component based on zirconia or ceria. Furthermore, the use of nickel-ceramic anodes "by default" is so established in the SOFC field that all other anode materials are considered alternatives.

There are many reasons for the high demand for nickel ceramic anodes:

– ease of manufacture and low cost;

– high catalytic activity of nickel for the hydrogen oxidation reaction, which, according to Setoguchi et al. [14] is higher than that of iron, ruthenium, manganese, and cobalt. Later, Rossmeisl et al. [15] using density functional theory (DFT) also showed that it is nickel that has the highest activity compared to other metals: Mn, Fe, Co, Cu, Ru, Pd, Ag, Pt, Au (Figure 2);

– high electronic conductivity, which depends on the nickel/ceramic ratio and for the most common weight

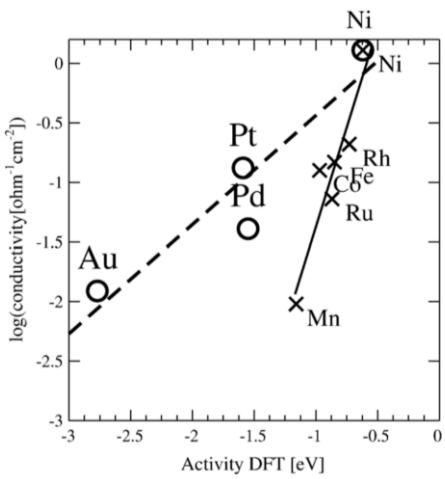

Figure 2 The experimental activity versus the activity predicted from theory [15].

ratio of 1/1 wt. % can reach values of about 1000 S/cm at SOFC operating temperatures [16-18];
– the thermal expansion of nickel-ceramic anodes (about $12.5 \cdot 10^{-6}$ 1/K [19]) is close to that of electrolytes and can be changed within a small range by varying the nickel/ceramic ratio;
– the porosity of the anode is always non-zero because the nickel-ceramic electrode is formed in an oxidizing atmosphere and the nickel in it as oxide, after the transition to a reducing atmosphere the nickel oxide is reduced to the metal, which leads to a decrease in its particle volume and, consequently, to an increase in the porosity of the anode.

Disadvantages of nickel-ceramic anodes are degradation of their characteristics over time, especially in atmospheres with high water partial pressures [20, 21], chemical interaction with highly conductive electrolytes based on lanthanum gallate [22, 23] and formation of carbon during operation with hydrocarbon fuels [24, 25], which leads to a decrease in the anode activity. Because of these drawbacks, especially carbon formation, new alternative anode materials have been researched and developed in recent years. Perhaps the first of these was a copper-ceria-based anode. Despite high carbon formation tolerance [26, 27], these materials have not been widely used because of their low activity to hydrogen oxidation, low activity to break C-C bonds in hydrocarbons, and fast degradation under SOFC operating conditions.

Other carbon tolerant anode studies have focused on oxide anode materials based on chromites, titanates, and lanthanum chromite-manganites. For example, more than a hundred different compositions of oxide anodes are described in Kolotygin's Ph.D. Thesis [28]. However, almost all proposed oxide anodes have a number of drawbacks: low electrical conductivity in reducing atmospheres [29, 30], low electrochemical activity [31, 32], the need to perform synthesis at low oxygen partial pressures (sometimes in a hydrogen atmosphere), high temperature reduction to obtain a single phase composition [33, 34]. As a result, the use of these materials as SOFC anodes is inappropriate. Recently, studies have been carried out on anode materials based on complex oxides, which can be considered as a real alternative to nickel-ceramic anodes [35–38].

2. Representation of electrode processes and rate-determining steps

Based on common ideas about the mechanisms of electrode processes in systems with solid oxygen-conducting electrolytes, the pathway of electrode oxygen reduction reactions at the cathode can be written in general terms as:
– diffusion of oxygen in the gas phase;
– oxygen adsorption on the cathode surface;
– oxygen ionization;
– bulk or surface diffusion of oxygen ion to the cathode/electrolyte boundary.

For the oxidation of hydrogen at the anode:
– hydrogen diffusion in the gas phase;
– hydrogen adsorption (dissociative adsorption);
– diffusion of adsorbed forms of hydrogen to the reaction area;
– oxidation of adsorbed hydrogen form by oxygen ion (charge transfer stage).
– desorption of hydrogen oxidation products, i.e. water;
– diffusion of water in the pores of the electrode to the gas phase.

It is reasonable to assume that each of the steps described above has its own rate, and that the step with the slowest rate (i.e., the rate-determining step) determines the rate of the overall electrode reaction. However, it should be noted that this is true for electrochemical systems in which the processes described above occur sequentially. In some electrochemical systems, when processes running parallel, the electrode reaction stage with the slowest rate can be bypassed by faster processes and have a less noticeable effect on the electrode reaction rate [39–43].

2.1. Oxygen reduction kinetics

One of the first studies on electrode reaction kinetics in systems with solid electrolytes was focused on metal electrodes in contact with zirconia based electrolytes [44–47]. However, complex behavior of electrode reactions with a multistep nature has been found even for these simple electrochemical systems. This is because the reaction pathway and the rate-determining steps depend on many factors, including the properties of the electrode and electrolyte materials, the electrode morphology, the gas phase composition, the thermal and electrochemical background of the samples, etc. [48–51]. It follows from equations 1 and 2 the most likely area for electrochemical reactions involving gaseous components is the three-phase boundary (TPB) gas/electrode/electrolyte [44, 52, 53]. The effect of the three-phase boundary on the rate of oxygen electroreduction was first shown by Karpachev et al. on the example of a platinum electrode formed on YSZ electrolyte [54]. Further understanding of the electrode reaction kinetics in the Pt/YSZ system allowed to determine that oxygen reduction is not limited by the charge transfer step, while changes in the concentration of oxygen adsorbed on platinum can significantly affect its rate [55–58]. Later, Mizusaki et al. showed that the rate-determining stage of oxygen reduction can depend on the

temperature range in which the system is studied [59, 60]. Thus, at temperatures below 500 °C, dissociative adsorption of oxygen on the platinum surface is the limiting stage of oxygen reduction; at higher temperatures – surface diffusion of atomic oxygen to the three-phase boundary. The authors also note that the charge transition stage does not limit the oxygen reduction rate. Further studies of oxygen adsorption processes on the platinum surface showed that the degree of coverage of the platinum surface with adsorbed atomic oxygen also plays a significant role in electrode kinetics, for example, the minimum of polarization resistance is realized when the degree of coverage of the platinum surface with adsorbed oxygen is 0.5 [61–67]. The key role of oxygen adsorption on the surface of platinum is also mentioned by Vayenas et al. [68–70], Chao et al. [71] and Kuzin et al. [72, 73]. It is also worth mentioning Glumov's hypothesis [74], which considers the reduction of oxygen at the two-phase electrolyte/gas interface. However, considering the low electron concentration in the YSZ electrolyte in oxidizing atmospheres, this assumption is unlikely, but it is quite valid for electrolytes in which the electron concentration is high. Later, Bronin [75] studied the Pt/LSGM system and proposed a model with two parallel oxygen reduction reaction pathways. The limiting stage of one of them is the surface diffusion of atomic oxygen adsorbed on platinum to the three-phase boundary, and the other one is the diffusion of electron holes from the electrolyte/gas boundary to the three-phase boundary.

Probably, one more metallic electrode worth noting is the silver electrode. Its specific feature is that silver at high temperatures is able to dissolve oxygen in itself, and the mobility of dissolved oxygen is quite high. Taking this into account, it can be assumed that all necessary conditions for the reaction according to Equation 1 are possible at the two-phase electrode/electrolyte interface. According to the authors [76–78], it is the diffusion of oxygen in silver that is the rate-determining stage of oxygen reduction.

Studies of metal electrodes allowed the formation of basic concepts of oxygen reduction mechanisms, which were then transferred to more complex objects, i.e., oxide cathodes with mixed electron and oxygen ion conductivity.

To date, the most widely studied cathode material on the basis of mixed conductors is lanthanum strontium manganite (LSM). Despite the high hole conductivity, which according to [79, 80] can reach 100 S/cm, the level of oxygen-ion conductivity in LSM is low, about 10^{-7} S/cm at 800 °C [81–83]. This allows us to consider the pathway of oxygen electroreduction on the LSM cathode in analogy to the platinum electrode discussed above, namely the critical influence of the three-phase boundary length. Diffusion of adsorbed atomic oxygen [84–87] or adsorption of oxygen on the LSM cathode surface [85, 88, 89] is considered as the rate-determining stage of oxygen reduction on the LSM.

The phenomena discussed above mainly affect the properties of the material itself and the properties of its surface, but in the case of oxygen electroreduction, oxygen diffusion in the gas phase and in the pores of the cathode will also play an important role. Molecular oxygen diffusion usually begins to limit the rate of the electrode reaction at low oxygen partial pressures [44, 90]. According to Mitterdorfer et al. [91, 92] for the Pt/YSZ cathode system, the oxygen gas diffusion begins to limit the cathode process at $pO_2 = 10^{-3}$ atm and below. For the $La_{0.6}Sr_{0.4}Fe_{0.8}Co_{0.2}O_{3-\delta}/Ce_{0.9}Gd_{0.1}O_{1.95}$ cathode system, according to [90], the influence of oxygen diffusion in the gas phase becomes noticeable already at $pO_2 = 0.1$ atm. In addition to the oxygen partial pressure, the resistance of the diffusion stage of the cathode reaction is also determined by the cathode microstructure [48, 93]. For example, using numerical simulations, Ni et al. showed that for a cathode with a porosity of 40 %, the effect of gas diffusion can occur even in an air atmosphere ($pO_2 = 0.21$ atm) if the electrode particle size is less than 0.2 μm [93].

To conclude our consideration of the oxygen electroreduction process at the TTE cathode, we should note the model that was first proposed by Adler et al. [90] and considers the cathode reaction as a pair of coupled processes: interphase exchange of oxygen of the electrode with oxygen of the gas phase and transport of the oxygen ion in the volume of the cathode material (Figure 3). According to this model, the resistance of the electrode process (the authors call it chemical resistance R_{chem}) can be written as:

$$R_{chem} = \left(\frac{RT}{2F^2}\right)\sqrt{\frac{\tau}{(1-\varepsilon)c_v\, D_v a r_0(\alpha_f+\alpha_b)}}, \qquad (4)$$

where τ – is the tortuosity factor, ε – is the porosity of the electrode, c_v – is the concentration of oxygen vacancies, D_v – is the vacancy diffusion coefficient, a – is the specific electrode surface, r_0 – is the exchange flux density (analogous to the exchange current density), α_f and α_b – are constants. Since the publication of this model, it has attracted a lot of attention of researchers, because it allows relating cathode microstructure parameters, results of direct measurements of oxygen diffusion coefficient by isotope exchange methods [94] and impedance spectroscopic studies under the assumption of

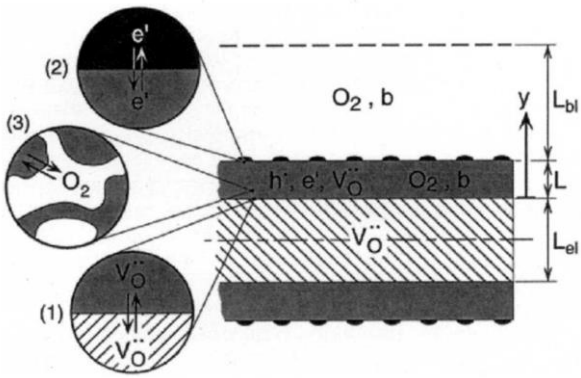

Figure 3 The one of the representations of the oxygen reaction [90].

interpretation of impedance spectra using Gerischer impedance [95], which as an admittance can be written as

$$Y_G = Y_0\sqrt{K_G + j\omega}, \quad (5)$$

where Y_G – is Gerischer admittance, Y_0 – is the frequency-independent part of the Gerischer admittance related to ion transport, K_G – is the Gerischer constant related to the rate of interphase exchange, j – is the imaginary unit, ω – is the circular frequency.

In [96] the oxygen reduction reaction on $Sr_{2(1.95)}Fe_{1.5}Mo_{0.5}O_{6-\delta}$ electrodes was studied by impedance spectroscopy with the subsequent interpretation of the data using the concepts outlined in the Adler et al. model. The high-frequency stage of the electrode reaction was described by the Gerischer impedance and is associated with oxygen surface exchange and oxygen diffusion in the electrode material. The low-frequency stage is attributed to the Knudsen diffusion in the pores of the electrode. Based on the Adler et al. model, the qualitative correlation between the impedance data and oxygen isotopic exchange data for $Sr_2Fe_{1.5}Mo_{0.5}O_{6-\delta}$ was demonstrated for the first time in [96]. On the other hand, Almar et al. [97] showed that in the $Ba_{0.5}Sr_{0.5}Co_{0.8}Fe_{0.2}O_{3-\delta}/Ce_{0.9}Gd_{0.1}O_{2-\delta}$ electrode system the oxygen reduction rate is determined only by the rate of oxygen interphase exchange with the gas phase, no Gerischer-like behavior was detected for the impedance spectra.

2.2. Hydrogen oxidation at the metal anodes

As in the case of an oxygen reduction reaction, hydrogen oxidation in systems with solid oxide electrolytes was first studied on a platinum electrode in contact with YSZ electrolyte. One of the first detailed studies of the Pt/YSZ system in $H_2 + H_2O$ gas mixtures showed that the rate-determining stage of the electrode process is the chemical interaction between the partially reduced solid electrolyte and water [98–100]. It was later shown that the hydrogen reaction on both platinum and nickel electrodes is controlled by charge transfer and heterogeneous processes, presumably water adsorption at the three-phase interface [101]. In the studies of Fernandez et al. [102, 103], it was shown that the electrode process on the nickel electrode can depend on the electrode potential. At an electrode potential more positive than –1.2 V (vs. air electrode), water reduction is limited by adsorption-desorption stages of gas phase components or by diffusion of adsorbed particles. At an electrode potential of negative –1.2 V, water reduction is possible on the electrolyte surface due to the appearance of electron charge carriers in it.

In the case of the Ni/YSZ electrochemical system, the electrode reaction rate in the $H_2 + H_2O$ medium is also proportional to the length of the three-phase boundary, which was first shown by Kuzin on gas-tight nickel electrodes [104]. Later, these results were confirmed by Mizusaki et al. [105]. Later, Nakagawa et al. showed that the electrode reaction rate of water reduction does not depend on the thickness of a dense nickel electrode in the $H_2 + H_2O$ mixture [106]. It follows that the diffusion of water/hydrogen in the nickel volume has no appreciable effect on the electrode reaction rate. Since the rate of electrochemical reaction on metal electrodes depends on the length of the three-phase boundary, it is necessary to use composite powders to increase the activity of the electrodes, since in this case the three-phase boundary extends into the bulk of the electrode [107–109]. In the case of composite electrodes, phenomena localized at the electrode/electrolyte interface play an important role in the kinetics of the electrode reaction. One of these phenomena is the so-called spillover effect. Let us analyze this phenomenon in more detail.

2.2.1. Hydrogen spillover effect

The mechanism of electrode reaction involving hydrogen spillover was first proposed by Mogensen et al. by interpreting electrochemical impedance spectra of a nickel-ceramic anode in $H_2 + H_2O$ [110]. It was assumed that the high-frequency circle of the spectrum at low partial pressures of hydrogen (0.05 – 0.3 atm.) was related to proton transport. The low-frequency circle at high pH_2 (0.5 – 0.97 atm) was attributed to the stage of water formation on the YSZ electrolyte surface.

Within the framework of this mechanism, the anodic process is described by the following stages.

1. Adsorption of molecular hydrogen on the nickel surface with subsequent dissociation:

$$H_{2(gas)} + 2[\quad]_{Ni} = 2H_{Ni}, \quad (6)$$

where $[\quad]_{Ni}$ – an active site of hydrogen adsorption on nickel surface.

2. Ionization of atomic hydrogen on the surface of nickel:

$$H_{Ni} = H^{+}{}_{Ni} + e^{-}{}_{Ni}. \quad (7)$$

3. Proton diffusion along the nickel surface to the three-phase boundary (TPB).

4. Proton spillover to the surface of YSZ electrolyte and interaction with oxygen ion:

$$H^{+}{}_{YSZ} + O^{2-}{}_{YSZ} = OH^{-}{}_{YSZ}. \quad (8)$$

5. Water formation and its desorption into the gas phase.

Later, de Boer proposed a different, but rather close to the one discussed above, mechanism of hydrogen oxidation [111]. An important difference between the De Boer and Mogensen mechanisms is that the hydrogen adsorbed on the nickel surface (Equation 6) first reacts with the oxygen ion to form a protonated oxygen ion in the oxygen sublattice of the YSZ electrolyte. The protonated ion then leaves the oxygen sublattice to the electrolyte surface where it reacts with a hydrogen atom to form water.

In contrast to the mechanisms proposed by Mogensen and de Boer, the mechanism of hydrogen oxidation proposed by Lee et al. [112], special attention is paid to the intermediate stage of hydrogen oxidation, namely, the charge transfer stage is considered in a two-stage configuration, and the pathway itself can be written as follows.

1. Dissociative adsorption of hydrogen on the nickel surface, similar to Equation 6.

2. Oxygen ion release from the YSZ sublattice of the electrolyte onto its surface:

$$O_{O}^{\times} = O^{2-} + V_{O}\ . \quad (9)$$

3. Two-stage charge transfer:

$$H_{Ni} + O^{2-}{}_{YSZ} = OH^{-}{}_{YSZ} + e^{-}{}_{Ni}, \quad (10)$$

$$H_{Ni} + OH^{-}{}_{YSZ} = H_2O_{YSZ} + e^{-}{}_{Ni}. \quad (11)$$

4. Desorption of water from the surface of YSZ electrolyte.

Jiang and Badwal proposed another mechanism for the anodic reaction, which makes it possible to explain the increase in the activity of nickel-ceramic anodes in $H_2 + H_2O$ mixtures with increasing partial pressure of water in the gas phase [113, 114]. In contrast to the previous mechanisms, where hydrogen spillover from the nickel surface to the electrolyte surface is considered, in their model the authors, in addition to spillover, consider the possibility of water adsorption on the nickel surface.

1. Dissociative adsorption of hydrogen on nickel surface:

– for dry hydrogen adsorption proceeds similarly to Equation 6;

– for wet hydrogen, a parallel adsorption mechanism is considered:

$$H_2O_{(gas)} + [\quad]_{Ni} = (Ni-O)_{Ni} + H_{2(gas)}, \quad (12)$$

$$H_{2(gas)} + 2[\quad]_{Ni} = 2H_{Ni}, \quad (13)$$

$$H_{Ni} + (Ni-O)_{Ni} \rightarrow [\quad]_{Ni} + H(Ni-O). \quad (14)$$

2. Surface diffusion.

– for dry hydrogen, diffusion of adsorbed hydrogen across the nickel surface to the three-phase boundary;

– for wet hydrogen, diffusion of H(Ni-O) complex to the three-phase boundary.

3. Hydrogen or hydroxyl complex spillover to the surface of the YSZ electrolyte:

$$H_{Ni} \text{ and / or } H(Ni-O) = H_{YSZ}. \quad (15)$$

4. Charge transfer stage and water formation near the three-phase boundary:

$$O_{O\ (YSZ)}^{\times} + 2H_{YSZ} = H_2O_{(gas)} + V_{O\ \ (YSZ)} + 2e'_{YSZ}. \quad (16)$$

5. Electron transfer from the electrolyte to the nickel.

The main feature of this mechanism is the presence of an active site on the nickel surface capable of splitting oxygen from the water molecule. In their mechanism, Jiang and Badwal abandoned consideration of adsorbed forms of water. Moreover, the authors assume that dissociative adsorption of hydrogen occurs quickly at SOFCs operating temperatures and that the coverage of the nickel surface by adsorbed forms of hydrogen is low, hence, for dry hydrogen, surface diffusion will be the rate-determining step. Despite the fact that the number of active sites on the nickel surface will decrease due to water adsorption when water appears in the fuel mixture, the overall rate of the anodic reaction will increase due to faster diffusion of hydrogen across the anode surface through the formation of H(Ni-O) complexes. The authors consider stages 3 (Equation 15) and 4

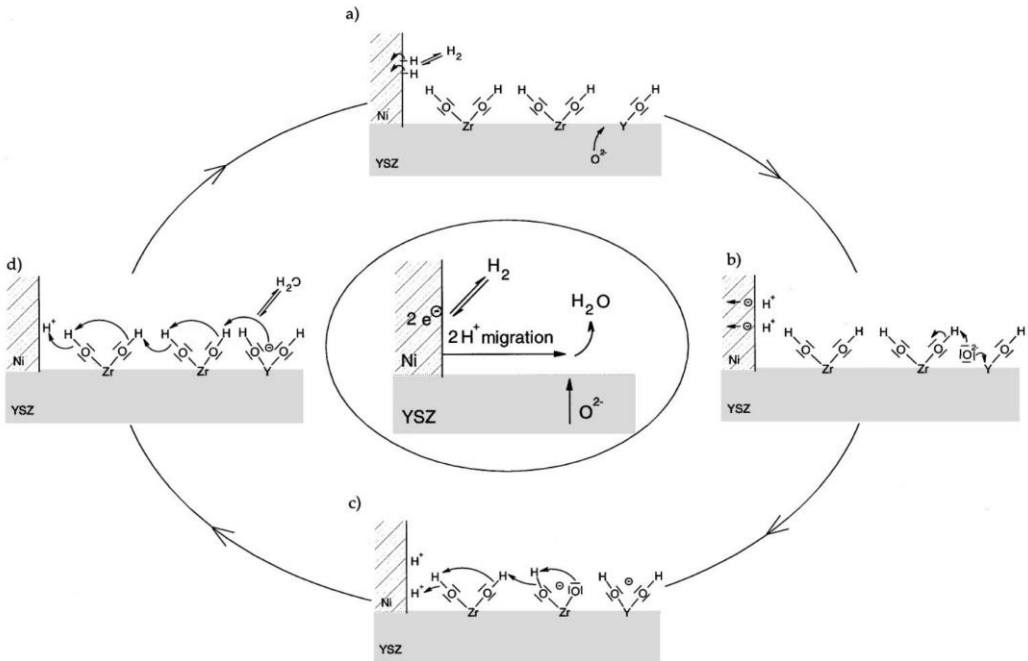

Figure 4 Image of the mechanism of hydrogen oxidation in the presence of water [115].

(Equation 16) to be the rate-determining stages in a humid hydrogen atmosphere.

Later, Bieberle et al. [115] performed impedance spectroscopic studies of a screen-printed nickel electrode and also postulated the catalytic role of water in the hydrogen oxidation process. The authors have considered hydrogen spillover to the YSZ electrolyte through the mechanism schematically shown in Figure 4. The authors also say that in dry hydrogen the number of electrochemically active centers near the three-phase boundary is limited. In the presence of water in the gas mixture, the surface of the YSZ electrolyte is covered with its adsorbed forms, which promote proton transport to (from) the nickel surface.

2.2.2. Oxygen spillover

When oxygen spillover in the hydrogen oxidation mechanism is considered, it is implied that oxygen ions migrate from the YSZ electrolyte to the nickel surface near the three-phase interface, where they react with adsorbed forms of hydrogen. In contrast to the above mechanisms with hydrogen jumping, in this case the dissociative adsorption of hydrogen and the desorption of water formed as a result of the electrochemical reaction occur on the nickel surface. The mechanism of anodic reaction considering oxygen spillover was first published by Mizusaki et al. [105] in studies of nickel electrodes.

Later, Bieberle et al. [116, 117] compared the results of impedance spectroscopic studies with calculated data for a model nickel electrode in $H_2 + H_2O$ mixtures and

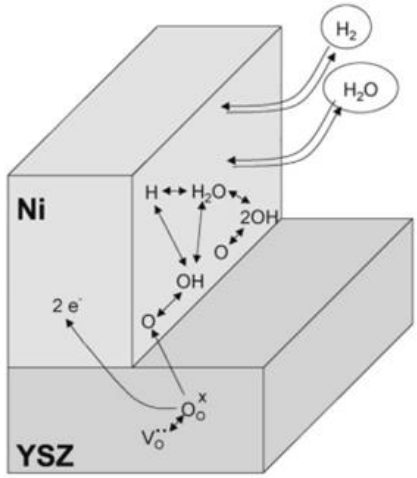

Figure 5 Mechanism of hydrogen electrooxidation in H_2+H_2O mixture at a nickel electrode in contact with YSZ electrolyte taking into account oxygen spillover [117].

proposed their own mechanism of the anodic reaction with the inclusion of the oxygen jump stage (Figure 5), based on the better convergence of experimental and calculated data.

The proposed anodic reaction pathway considers the following steps:

1. Adsorption/desorption of water and hydrogen on the nickel surface:

$$H_{2(gas)} + 2[\quad]_{Ni} = 2H_{Ni}, \tag{17}$$

$$H_2O_{(gas)} + [\quad]_{Ni} = H_2O_{Ni}. \tag{18}$$

2. Reactions on the surface of nickel:

$$O_{Ni} + H_{Ni} = OH_{Ni}, \quad (19)$$

$$H_2O_{Ni} + O_{Ni} = 2OH_{Ni}, \quad (20)$$

$$H_2O_{Ni} + [\quad]_{Ni} = OH_{Ni} + H_{Ni}. \quad (21)$$

3. The stage of oxygen spillover from the YSZ volume to the nickel surface:

$$O_{O\,(YSZ)}^{\times} + [\quad]_{Ni} = O_{Ni} + V_{O\ (YSZ)} + 2e_{Ni}^{'}. \quad (22)$$

However, this mechanism was proposed taking into account some assumptions: the surface of the YSZ electrolyte was considered electrochemically inert, reaction rates were calculated without taking into account the degree of coverage of the anode surface by adsorbed particles, surface diffusion was considered very fast, and gas-diffusion transport was not considered at all. In addition, the oxygen overshoot stage does not address the very nature of the fuel gas and can be applied to almost any electrooxidizable gaseous substance to some degree.

It should also be noted that later combined mechanisms for the anodic reaction at the nickel electrode in $H_2 + H_2O$ mixtures that already included several flow stages were proposed. For example, Bessler et al. in [118] presented the results of thermodynamic modeling of the anodic process on a nickel anode in contact with YSZ electrolyte and considered three different reaction routes taking into account oxygen and hydrogen spillover, and five different reactions are considered as charge transfer stages. The results obtained by the authors unambiguously showed an acceleration of the anodic reaction when the partial pressure of water in the $H_2 + H_2O$ mixture increased, with the charge transfer stage being the hydrogen spillover from the nickel surface to the hydroxyl group on the YSZ electrolyte.

2.3. Oxidation of carbon monoxide on metal anodes

The study of the process of carbon monoxide oxidation is of no less interest from the point of view of studying the anodic reaction routes. This is due to the fact that, like hydrogen, carbon monoxide is capable of direct oxidation on the anodes of SOFC. Also important is the fact that hydrocarbons after steam-water or carbon dioxide conversion, as well as biogas, are complex gas mixtures, the oxidizable components of which are mainly hydrogen and CO. Many works have been devoted to the study of CO oxidation on platinum, nickel, and nickel-ceramic anodes, but in all of them the authors note a lower electrochemical activity of the anodes when carbon monoxide is used as a fuel gas compared to hydrogen [119–122].

Perhaps one of the first efforts to explain the CO oxidation pathway on a porous platinum electrode in contact with YSZ electrolyte was made by Etsell et al. [123] in 1971, and the authors proposed two pathways of CO oxidation.

Pathway 1. Output of oxygen in atomic form from the electrolyte volume to the three-phase boundary (charge transfer stage according to Equation 23) with its subsequent interaction with the CO molecule to form carbon dioxide according to Equation 24.

$$O_{O\,(YSZ)}^{X} + [\quad]_{Pt/YSZ} = O_{Pt/YSZ} + V_{O\ (YSZ)}^{\bullet\bullet} + 2e_{Pt}^{'}, \quad (23)$$

$$CO_{(gas)} + O_{(Pt/YSZ)} = CO_{2(gas)} + [\quad]_{Pt/YSZ}. \quad (24)$$

The second pathway was the oxidation process of CO by oxygen in the YSZ sublattice of the electrolyte (Equation 25).

$$CO_{(gas)} + O_{O\,(YSZ)}^{X} = CO_{2(gas)} + V_{O\ (YSZ)}^{\bullet\bullet} + 2e_{Pt}^{'}. \quad (25)$$

A feature of the above-mentioned routes is that the authors refused to consider adsorbed forms of CO on the anode surface, which, taking into account modern ideas about electrode processes, is rather controversial.

At present, the presence of adsorbed CO molecules on the anode surface as well as their key role in the electrode reaction are no longer in doubt and the CO adsorption stage is considered as one of the main ones. Thus, for example, Lauvstad et al. [124] suggest that CO oxidation occurs by the following route:

– CO adsorption on the nickel surface;
– surface diffusion of adsorbed CO to the three-phase boundary;
– diffusion of oxygen ion to the three-phase boundary in YSZ electrolyte;
– one- or two-stage charge transfer with the formation of CO_2.

The authors note that the rate-determining stage is the process of oxidation of adsorbed CO by oxygen ions, i.e., the charge transfer stage, but at low *p*CO the gas diffusion stage can limit the rate of the anodic reaction.

Matsuzaki et al. [120] studied the process of CO oxidation at the interface of porous Ni-YSZ anode and YSZ electrolyte and concluded that the low rate of CO electrooxidation (compared to hydrogen oxidation) can be related to the surface diffusion of adsorbed CO molecules at 750 °C, and at 1000 °C, the authors call two

rate-determining stages: surface diffusion of CO and charge transfer stage.

Note also the previously mentioned work by Somov et al. [125], in which the authors considered CO oxidation on metal (Ni, Pt, Pd, Cu, Ag) electrodes impregnated (modified) with cerium oxide. In this work, the authors emphasize the key role of cerium oxide particles, assuming that the adsorption of carbon monoxide occurs exclusively on their surface and the stage of charge transfer, i.e., CO oxidation is also localized on the mixed conductor particles. The nature of metals and their catalytic activity have not been considered by the authors.

2.4. Oxidation of hydrogen and carbon monoxide on oxide anodes based on strontium ferrite and molybdate

Mechanisms of hydrogen and carbon monoxide electrooxidation on oxide anodes have been studied to a much lesser extent compared to those on metal and metal-ceramic anodes. This may be due in part to the low degree of study of the electrode materials themselves and the depth of understanding of the electrochemical processes that occur in them.

Since as oxide anode materials it makes sense to use only oxides with high oxygen and electronic conductivities in reducing atmospheres, all necessary conditions for the hydrogen oxidation reaction according to Equation 2 can be realized at the two-phase electrode/gas interface. In this respect, the extent of the three-phase boundary will not play such a significant role as it was in the case of metallic or Ni-YSZ anodes. Let us consider the routes of the anodic process and rate-determining stages proposed by various author teams.

The route of hydrogen oxidation on $Sr(Ti_{0.3}Fe_{0.7})O_{3-\delta}$ anode was proposed by Zhu et al. [126]. As a total electrode reaction, the authors propose the process of hydrogen oxidation by oxygen located in the sublattice of strontium ferrite-titanium by the following reaction

$$CH_{2(gas)} + O^{X}_{O\ (anode)} = H_2O_{(gas)} + 2e'_{(anode)} + V_{O\ (anode)}, \quad (26)$$

which is realized in several stages:

– dissociative adsorption of hydrogen on the anode surface;

– oxygen transport from the anode volume to the surface;

– charge transfer stage with water formation on the anode surface;

– water desorption.

It is noteworthy that the proposed route well describes the experimental data of impedance spectroscopy and constant current measurements carried out by the authors. The authors note that, unlike Ni-YSZ anodes, where hydrogen adsorption occurs mainly on the metal surface, in an oxide anode it is possible over the entire electrode surface, and the previously proposed stages of the anodic reaction associated with hydrogen jump are not relevant for oxide anodes. The authors also note that charge transfer can occur in two stages. The first stage produces hydroxide ions and the second stage produces water. The authors call the hydrogen adsorption stage the rate-determining stage. It is worth noting that the authors made a number of assumptions when deriving this model of the electrode reaction: the anode surface was considered to consist entirely of oxygen ions only, and the authors also did not consider gas diffusion processes.

The inhomogeneity of the surface cation composition was taken into account when considering the mechanism of the anodic reaction by Chen et al. [127] on the example of $La_{0.3}Sr_{0.7}Fe_{0.7}Cr_{0.3}O_{3-\delta}$ anode. The authors consider the adsorption of hydrogen on the oxygen atom in its sublattice as the first stage of the anodic reaction, and the dissociation of hydrogen into atoms is considered without the participation of the strontium or lanthanum atom. Then the charge transfer stage with the formation of water and oxygen vacancy is considered, which is quite close to the mechanisms proposed in [128–130].

In [131], Ammal et al. using density functional theory (DFT) and microkinetic modeling calculated CO oxidation rates and gas synthesis on the surface of a $SrFe_{0.75}Mo_{0.25}O_{3-\delta}$ anode as a function of the Fe/Mo ratio, the concentration of oxygen vacancies on the anode surface, and when taking into account the inhomogeneity of the cationic composition of the surface. As a result of calculations, the authors concluded that CO molecules are oxidized at the anode much slower than hydrogen, and the rate-determining stages are the surface diffusion of CO or the stage of CO_2 desorption with the formation of oxygen vacancy and the stage of charge transfer. Also, according to their data, at simultaneous presence of H_2 and CO in fuel gas with CO content less than 50 vol. % at the anode will be mainly oxidized hydrogen. However, at CO contents above 85 vol. %, the anode behavior is practically similar to that of an anode in pure CO. In general, the considered routes for CO oxidation on oxide anodes do not differ much from the mechanisms of hydrogen oxidation discussed above and, as a rule, the charge transfer, adsorption, and surface diffusion stages of CO are proposed as rate-determining stages [132, 133]. By means of a complex approach to the impedance spectra analysis using the distribution of relaxation times and nonlinear least squares methods, it was determined that the CO oxidation is limited by three steps: CO adsorption (CO_2 desorption) at the electrode surface, oxygen hetero-exchange and the oxygen ion transport in the electrode

bulk. We assume that the charge transfer and the gas diffusion do not limit the CO oxidation reaction on the $Sr_2Fe_{1.5}Mo_{0.5}O_{6-\delta}$ electrode [134].

3. Conclusions

It follows from the literature review that certain successes have been achieved to date in the study of the mechanisms of electrode reactions of hydrogen and carbon monoxide oxidation on nickel and nickel-ceramic anodes. Electrode reactions on anodes made of oxides with a high level of mixed conductivity have been studied to a lesser extent, which may be due to the low stability of most of the known oxides in strongly reducing atmospheres.

At the same time, the literature analysis shows a great variety of proposed interpretations of electrode reactions. This is due to the fact that the nature of the rate-determining stages of the electrode reaction depends not only on the chemical composition of the electrode material but also on its microstructure, the nature of the supporting electrolyte, the quality of the electrode/electrolyte boundary, the conditions of electrode formation, its prehistory, and external conditions. In this connection, the study of electrode processes even for nickel-ceramic electrodes does not lose its relevance. More relevant are studies of anodes exhibiting high electrochemical activity, for example, nickel-ceramic anodes modified with cerium oxide, and oxide electrodes stable in reducing media, for example, on the basis of strontium ferrite-molybdates, which were mentioned in the literature review.

Studies in the field of degradation phenomena of nickel-ceramic anodes, especially in atmospheres with high partial pressure of water, are relevant, since the nature of the processes leading to deterioration of electrical and electrochemical characteristics of nickel-ceramic electrodes in time is not unambiguously established. Close attention to studies of rate-determining stages of electrode reactions and processes leading to degradation of electrode characteristics is due to the possibility of purposeful influence on them in order to improve electrode characteristics and reduce the rate of degradation processes.

Supplementary materials

No supplementary materials are available.

Funding

This research had no external funding.

Acknowledgments

None.

Author contributions

Denis Osinkin: Conceptualization; Data curation; Writing – original draft; Writing – Review & Editing.

Conflict of interest

The authors declare no conflict of interest.

Additional information

Denis Osinkin, Scopus Author ID: 26536496100; Orcid: 0000-0001-6396-8551; Web of Science ResearcherID: D-8913-2017.

References

1. Schottky W, Über stromliefernde Prozesse im Konzentrationsgefälle fester Elektrolyte, Wiss. Veröff. Siemens-Werken, **14 (2)** (1935) 1–19.

2. Nernst W, assignor to George Westinghouse, of Pittsburg, Pennsylvania, Electrical glow light. United States patent US623811A. 1899 Apr 25.

3. Nernst W, Uber die elektrolvtische Leitung Fester Korper bei sehr hohen Temperaturen, Z. Elektrochem. **6 (2)** (1899) 41-43. https://doi.org/10.1002/bbpc.18990060205

4. Bauer E, Brunner R, Uber die Eisenoxyd-Kathode in der Kohle-Luft-Kette, Z, Elektrochem. **43 (9)** (1937) 725–727. https://doi.org/10.1002/bbpc.19370430902

5. Bauer E, Preis H, Uber Brennstoff-Ketten mit Festleitern, Z, Elektrochem. **43 (9)** (1937) 727–732. https://doi.org/10.1002/bbpc.19370430903

6. Wagner C, Über den mechanismus der elektrischen Stromleitung im Nernststift, Naturwissenschaften, **31** (1943) 265–268. https://doi.org/10.1007/BF01475685

7. Weissbart J, Ruka R, A solid electrolyte fuel cell, J. Electrochem. Soc. **109** (1962) 723–726. https://doi.org/10.1149/1.2425537

8. Zhu B, Mi Y, Xia C, Wang B, et al., A nanoscale perspective on solid oxide and semiconductor membrane fuel cells: materials and technology, Energy Mater. **1** (2021) 100002. https://doi.org/10.20517/energymater.2021.03

9. Filonova E, Pikalova E, Overview of Approaches to Increase the Electrochemical Activity of Conventional Perovskite Air Electrodes, Materials, **16 (14)** (2023) 4967. https://doi.org/10.3390/ma16144967

10. Porotnikova N, Osinkin D, Recent advances in heteroatom substitution $Sr_2Fe_{1.5}Mo_{0.5}O_{6-\delta}$ oxide as a more promising electrode material for symmetrical solid-state electrochemical devices: A review, Electrochem. Mater. Technol. **1** (2022) 20221003. https://doi.org/10.15826/elmattech.2022.1.003

11. Saheli B, Gurpreet K, Gary P, Sarbjit G, A critical review on cathode materials for steam electrolysis in solid oxide electrolysis, Int. J. Hydrogen Energy, **48 (34)** (2023) 12541–12570. https://doi.org/10.1016/j.ijhydene.2022.11.307

12. Hu S, Li J, Zeng Y, Pu J, et al., A mini review of the recent progress of electrode materials for low-temperature solid oxide fuel cells, Phys. Chem. Chem. Phys. **25** (2023) 5926–5941. https://doi.org/10.1039/D2CP05133H

13. Pikalova EY, Kalinina EG, Pikalova NS, Filonova EA, High-Entropy Materials in SOFC Technology: Theoretical Foundations for Their Creation, Features of Synthesis, and Recent Achievements, Materials, **15 (24)** (2022) 8783. https://doi.org/10.3390/ma15248783

14. Setoguchi T, Okamoto K, Eguchi K, Arai H, Effects of anode material and fuel on anodic reaction of solid oxide fuel cells, J. Electrochem. Soc. 139(10) (1992) 2875–2880. https://doi.org/10.1149/1.2068998

15. Rossmeisl J, Bessler WG, Trends in catalytic activity for SOFC anode materials, Solid State Ionics, **178** (2008) 1694–1700. https://doi.org/10.1016/j.ssi.2007.10.016

16. Lee DS, Lee JH, Kim J, Lee HW, et al., Tuning of the microstructure and electrical properties of SOFC anode via compaction pressure control during forming, Solid State Ionics, **166** (2004) 13–17. https://doi.org/10.1016/j.ssi.2003.10.003

17. Corbin SF, Qiao X, Development of Solid Oxide Fuel Cell Anodes Using Metal-Coated Pore-Forming Agents, J. Am. Ceram. Soc. **86** (2003) 401–406. https://doi.org/10.1111/j.1151-2916.2003.tb03312.x

18. Koide H, Someya Y, Yoshida T, Maruyama T, Properties of Ni/YSZ cermet as anode for SOFC, Solid State Ionics, **132** (2000) 253–260. https://doi.org/10.1016/S0167-2738(00)00652-4

19. Osinkin DA, Bronin DI, Beresnev SM, Bogdanovich NM, et al., Thermal expansion, gas permeability, and conductivity of Ni-YSZ anodes produced by different techniques, J. Solid State Electrochem. **18** (2014) 149–156. https://doi.org/10.1007/s10008-013-2239-4

20. Osinkin DA, Long-term tests of Ni-$Zr_{0.9}Sc_{0.1}O_{1.95}$ anode impregnated with CeO_2 in $H_2 + H_2O$ gas mixtures, Int. J. Hydrogen Energy, **41** (2016) 17577–17584. http://doi.org/10.1016/j.ijhydene.2016.07.136

21. Osinkin DA, Degradation of Ni-$Zr_{0.9}Sc_{0.1}O_{1.95}$ anode in $H_2 + H_2O$ at low temperature: Influence of nickel surface charge, Int. J. Hydrogen Energy, **43** (2018) 943–950. https://doi.org/10.1016/j.ijhydene.2017.11.071

22. Feng M, Goodenough JB, Huang K, Milliken C, Fuel cells with doped lanthanum gallate electrolyte, J. Power Sources, **63** (1996) 47–51. https://doi.org/10.1016/S0378-7753(96)02441-X

23. Huang K, Tichy R, Goodenough JB, Superior Perovskite Oxide-Ion Conductor; Strontium- and Magnesium-Doped LaGaO3: I. Phase Relationships and Electrical Properties, J. Am. Ceram. Soc. **81** (1998) 2565–2575. https://doi.org/10.1111/j.1151-2916.1998.tb02662.x

24. Hua D, Li G, Li H, Zhang X, et al., Investigation of carbon formation on Ni/YSZ anode of solid oxide fuel cell from CO disproportionation reaction, Int. Comm. Heat and Mass Tran. **91** (2018) 23–29. https://doi.org/10.1016/j.icheatmasstransfer.2017.11.014

25. Jia L, Wang X, Hua B, Li W, et al., Computational analysis of atomic C and S adsorption on Ni, Cu, and Ni-Cu SOFC anode surfaces, Int. J. Hydrogen Energy, 37 (2012) 11941–11945. https://doi.org/10.1016/j.ijhydene.2012.05.041

26. Ye X, Zhou J, Zeng SR, Wen TL, et al., Research of carbon deposition formation and judgment in Cu-CeO_2-ScSZ anodes for direct ethanol solid oxide fuel cells, Int. J. Hydrogen Energy, **37** (2012) 505–510. https://doi.org/10.1016/j.ijhydene.2011.09.017

27. An S, Lu C, Worrell WL, Vohs JM, Characterization of Cu–CeO_2 direct hydrocarbon anodes in a solid oxide fuel cell with lanthanum gallate electrolyte, Solid State Ionics, **175** (2004) 135–138. https://doi.org/10.1016/j.ssi.2004.09.029

28. Kolotygin V. Materiais a Base de Oxidos com Estrutura do Tipo Perovskite e Compositos como Anodos de PCES Propriedades Funcionais e Comportamento Eletroquimico em Celulas com Eletrolitos Solidos a Base de Galatos e Silicatos [PhD Thesis]. Aveiro (Portugal): Universidade de Aveiro, Portugal; 2015. 259 p.

29. Fu QX, Tietz F, Stover D, $La_{0.4}Sr_{0.6}Ti_{1-x}Mn_xO_{3-\delta}$ perovskites as anode materials for solid oxide fuel cells, J. Electrochem. Soc. **153** (2006) D74–D83. https://doi.org/10.1149/1.2170585

30. Azad AK, Eriksson GG, Irvine JTS, Structural, magnetic and electrochemical characterization of $La_{0.83}A_{0.17}Fe_{0.5}Cr_{0.5}O_{3-\delta}$ (A = Ba, Ca) perovskites, Mater. Res. Bull. **44** (2009) 1451–1457. https://doi.org/10.1016/j.materresbull.2009.03.008

31. Deleebeck L, Fournier JL, Birss V, Comparison of Sr-doped and Sr-free $La_{1-x}Sr_xMn_{0.5}Cr_{0.5}O_{3\pm\delta}$ SOFC Anodes, Solid State Ionics, **181** (2010) 1229–1237. https://doi.org/10.1016/j.ssi.2010.05.027

32. Tao SW, Irvine JTS, Phase Transition in Perovskite Oxide $La_{0.75}Sr_{0.25}Cr_{0.5}Mn_{0.5}O_{3-\delta}$ Observed by in Situ High-Temperature Neutron Powder Diffraction, Chem. Mater. **18** (2006) 5453–5460. https://doi.org/10.1021/cm061413n

33. Cascos V, Troncoso L, Alonso JA, Fernandez-Diaz MT, Design of new Ga-doped $SrMoO_3$ perovskites performing as anode materials in SOFC, Renew. Energy, **111** (2017) 476–483. https://doi.org/10.1016/j.renene.2017.04.023

34. Childs NB, Wesinstein A, Smith R, Sofie S, et al., Key Electrical conductivity of $Sr_{2-x}VMoO_{6-y}$ (x = 0.0, 0.1, 0.2) double perovskites, J. Appl. Phys. **113** (2013) 243506. https://doi.org/10.1063/1.4811715

35. Zamudio-García J, Caizan-Juanarena L, Porras-Vazquez JM, Losilla ER, Marrero-Lopez D, A review on recent advances and trends in symmetrical electrodes for solid oxide cells, J. Power Sources, 520 (2022) 230852. https://doi.org/10.1016/j.jpowsour.2021.230852

36. Zhu K, Luo B, Liu Z, Wen X, Recent advances and prospects of symmetrical solid oxide fuel cells, Ceram. Int. **48** (2022) 8972–8986. https://doi.org/10.1016/j.ceramint.2022.01.258

37. Ruiz-Morales JC, Marrero-Lo´pez D, Canales-Va´zquezc J, Irvine JTS, Symmetric and reversible solid oxide fuel cells, RSC Advances, **1** (2011) 1403–1414. https://doi.org/10.1039/C1RA00284H

38. Shu L, Sunarso J, Hashim SS, Mao J, et al., Advanced perovskite anodes for solid oxide fuel cells: A review, Int. J. Hydrogen Energy, **44** (2019) 31275–31304. https://doi.org/10.1016/j.ijhydene.2019.09.220

39. Hu H, Liu M, Interfacial polarization characteristics of Pt|$BaCe_{0.8}Gd_{0.2}O_3$|Pt cells at intermediate temperatures, J. Electrochem. Soc. **144** (1997) 3561–3567. https://doi.org/10.1149/1.1838048

40. Antonova EP, Bronin DI, Stroeva AYu, Polarization resistance of platinum electrodes in contact with proton-

conducting $La_{0.9}Sr_{0.1}ScO_{3-\delta}$, Russ. J. Electrochem. **50** (2014) 613–616. https://doi.org/10.1134/S1023193514070027

41. Liu M, Hu H, Effect of interfacial resistance on determination of transport properties of mixed-conducting electrolytes, J. Electrochem. Soc. **143 (6)** (1996) L109–L112. https://doi.org/10.1149/1.1836892

42. Poetzsch D, Merkle R, Maier J, Investigation of oxygen exchange kinetics in proton-conducting ceramic fuel cells: Effect of electronic leakage current using symmetric cells, J. Power Sources, **242** (2013) 784–789. https://doi.org/10.1016/j.jpowsour.2013.05.108

43. Antonova EP, Electro transfer and kinetics of electrode processes in systems with proton conducting electrolytes with perovskite structure [dissertation]. Yekaterinburg (Russia): Institute of High Temperature Electrochemistry; 2015. 132 p.

44. Murygin IV. Electrodnye process v tverdyh electrolitah [Electrode processes in solid electrolytes]. Nauka: Moskva; 1991. 350 p. Russian.

45. Fabry P, Kleitz M, Influence of the metal and the electrolyte composition on the characteristics of the oxygen electrode reaction on solid oxide electrolyte, J. Electroanal. Chem. Inter. Electrochem. **57** (1974) 165-177. https://doi.org/10.1016/S0022-0728(74)80020-3

46. Perfiliev MV, Palguev SF. K voprosy o kinetike electrodnyh processov v tverdih electrolitah [Toward a question on the kinetics of electrode processes in solid electrolytes]. Collection of scientific papers of the Institute of Electrochemistry, UFAN USSR. 1966. 157–167.

47. Wang DY, Nowick AS, Diffusion-Controlled Polarization of Pt, Ag, and Au Electrodes with Doped Ceria Electrolyte, J. Electrochem. Soc. **128** (1981) 55–63. https://doi.org/10.1149/1.2127387

48. Adler SB, Factors governing oxygen reduction in solid oxide fuel cell cathodes, Chem. Rev. **104** (2004) 4791–4844. https://doi.org/10.1021/cr020724o

49. Jiang SP, Activation, microstructure, and polarization of solid oxide fuel cell cathodes, J. Solid State Electrochem. **11** (2007) 93–102. https://doi.org/10.1007/s10008-005-0076-9

50. Steele BCH, Behaviour of porous cathodes in high temperature fuel cells, Solid State Ionics, **94** (1997) 239–248. https://doi.org/10.1016/S0167-2738(96)00510-3

51. Simner SP, Anderson MD, Pederson LR, Stevenson JW, Performance Variability of La(Sr)FeO_3 SOFC Cathode with Pt, Ag, and Au Current Collectors, J. Electrochem. Soc. **152** (2005) A1851–A1859. https://doi.org/10.1149/1.1995687

52. Kinoshita K. Electrochemical oxygen technology: Wiley-Interscience; New York. 1992. 448 p.

53. Bouwmeester HJN, Burgraaf AJ. Dense ceramic membranes for oxygen separation In: Burggraaf AJ, Cot L (eds) Fundamentals of inorganic membrane science and technology. Elsevier: Amsterdam; 1996. 435–528.

54. Karpachev SV, Filyaev AT, K voprosy electrohimicheskoy kinetiki v slychae tverdogo electrolita [Toward the question of electrochemical kinetics in the case of solid electrolyte, Electrohimiya, **2 (11)** (1966) 1330–1332.

55. Schouler E, Giroud G, Kleitz M, Applications selon Bauerle du trace des diagrammes d'admittance complex en électrochimie des solides. II. Étude de la conductivite de la zircone stabilisee a l'yttrium, J. Chim. Physiq. **70** (1973) 1309–1316. https://doi.org/10.1051/jcp/1973701309

56. Verkerk MJ, Burggraaf AJ, Oxygen transfer on substituted ZrO2, Bi_2O_3, and CeO_2 electrolytes with platinum electrodes. II. a-c impedance study, J. Electrochem. Soc. **130 (1)** (1983) 78–84. https://doi.org/10.1149/1.2119687

57. Verkerk MJ, Hammink MWJ, Burggraaf AJ, Oxygen transfer on substituted ZrO_2, Bi_2O_3, and CeO_2 electrolytes with platinum electrodes. I. Electrode resistance by d-c polarization, J. Electrochem. Soc. **130 (1)** (1983) 70–78. https://doi.org/10.1149/1.2119686

58. Bauerle JE, Study of solid electrolyte polarization by a complex admittance method, J. Phys. Chem. Solid. **30 (12)** (1969) 2657–2670. https://doi.org/10.1016/0022-3697(69)90039-0

59. Mizusaki J, Amano K, Yamauchi S, Fueki K, Electrode reaction at Pt, O_2(g)/stabilized zirconia interfaces. Part I: Theoretical consideration of reaction model, Solid State Ionics, **22** (1987) 313–322. https://doi.org/10.1016/0167-2738(87)90149-4

60. Mizusaki J, Amano K, Yamauchi S, Fueki K, Electrode reaction at Pt, O_2(g)/stabilized zirconia interfaces. Part II: Electrochemical measurements and analysis, Solid State Ionics **22** (1987) 323–330. https://doi.org/10.1016/0167-2738(87)90150-0

61. Kuzin BL, Komarov MA, Adsorption of O_2 at Pt and kinetics of the oxygen reaction at a porous Pt in contact with a solid oxide electrolyte, Solid State Ionics, **39** (1990) 163–172. https://doi.org/10.1016/0167-2738(90)90395-8

62. Wang DY, Nowick AS, Cathodic and anodic polarization phenomena at platinum electrodes with doped CeO2 as electrolyte. II. Transient overpotential and ac-impedance, J. Electrochem. Soc. **126 (7)** (1979) 1166–1172. https://doi.org/10.1149/1.2129236

63. Winnubst AJA, Scharenborg AHA, Burggraaf AJ, The electrode resistance of ZrO_2–Y_2O_3(–Bi_2O_3) solid electrolytes with Pt electrodes, Solid State Ionics, **14** (1984) 319–327. https://doi.org/10.1016/0167-2738(84)90116-4

64. Schwandt C, Weppner W, Kinetics of oxygen, platinum/stabilized zirconia and oxygen, gold/stabilized zirconia electrodes under equilibrium conditions, J. Electrochem. Soc. **144 (11)** (1997) 3728–3738. https://doi.org/10.1149/1.1838083

65. Wang DY, Nowick AS, Cathodic and anodic polarization phenomena at platinum electrodes with doped CeO_2 as electrolyte. I. Steady-state overpotential, J. Electrochem. Soc. **126 (7)** (1979) 1155–1165. https://doi.org/10.1149/1.2129235

66. Sasaki J, Mizusaki H, Yamauchi S, Fueki K, Studies on electrode processes of stabilized zirconia systems by complex impedance method, Bull. Chem. Soc. Japan **54 (6)** (1981) 1688–1692. https://doi.org/10.1246/bcsj.54.1688

67. Gür TM, Raistrick ID, Huggins RA, Steady-state d–c polarization characteristics of the O_2, Pt/stabilized zirconia interface, J. Electrochem. Soc. **127 (12)** (1980) 2620–2628. https://doi.org 10.1149/1.2129532

68. Vayenas CG, Michaels VN, On the stability limit of surface platinum oxide and its role in oscillation phenomena of platinum catalyzed oxidations, Surf. Sci. **120 (1)** (1982) L405–L408. https://doi.org/10.1016/0039-6028(82)90265-5

69. Vayenas CG, Ioannides A, Bebelis S, Solid electrolyte cyclic voltammetry in situ investigation of catalyst surfaces, J. Catal. **129 (1)** (1991) 67–87. https://doi.org/10.1016/0021-9517(91)90010-2

70. Yentekakis IV, Neophytides S, Vayenas CG, Solid electrolyte aided study of the mechanism of CO oxidation on polycrystalline platinum, J. Catal. **111 (1)** (1988) 152–169. https://doi.org/10.1016/0021-9517(88)90074-7

71. Chao T, Walsh KJ, Fedkiw PS, Cyclic voltammetric study of the electrochemical formation of platinum oxide in a Pt/yttria-stabilized zirconia cell, Solid State Ionics, **47 (3–4)** (1991) 277–283. https://doi.org/10.1016/0167-2738(91)90250-F

72. Kuzin BL, Komarov MA, Termodinamika kislorodnogo electrode iz poristoy platiny v kontakte s tverdim oksidnim electrolitom pri visokih davleniyah kisloroda [Thermodynamics of porous platinum oxygen electrode in contact with solid oxide electrolyte at high oxygen pressures] Electrohimiya, **29 (11)** (1993) 1374–1379.

73. Kuzin BL, Komarov MA, Opredelenie nizhney granicy T, Po2-polya termodinamicheskih pokazaniy kislorodnogo electrode iz porispoy platiny v kontakte s electrolitom na osnove dioksida zirkoniya [Determination of the lower limit of T, Ro2-field thermodynamic readings of the oxygen electrode made of porous platinum in contact with zirconium dioxide electrolyte] Electrohimiya, **27 (9)** (1991) 1128–1132.

74. Glumov MV, Polarization of porous platinum electrodes in a solid-electrolyte cell in oxygen atmosphere, Soviet electrochemistry, **22 (2)** (1986) 207–211.

75. Bronin DI, Kinetics of electrode processes in electrochemical systems with solid oxide electrolytes [dissertation]. Yekaterinburg (Russia): Institute of high temperature electrochemistry; 2007. 283 p.

76. Perfiliev MV, Lobovikova NA, Vliyanie anodnoy polyarizacii na svoystva kontakta serebryanih electrodov s electrolitom $ZrO_2 + Y_2O_3$ [Effect of anodic polarization on the contact properties of silver electrodes with $ZrO_2 + Y_2O_3$ electrolyte] Electrohimiya, **20** (1984) 322–327.

77. Moghadam FK, Stevenson DA, Oxygen diffusion and solubility studies in Ag and Pt using ac impedance spectroscopy, J. Electrochem. Soc. **133 (7)** (1986) 1329–1332. https://doi.org/10.1016/10.1149/1.2108864

78. Jimenez R, Kloidt T, Kleitz M, Reaction-zone expansion and mechanism of the O_2, Ag/yttria-stabilized zirconia electrode reaction, J. Electrochem. Soc. **144 (2)** (1997) 582–585. https://doi.org/10.1149/1.1837451

79. Kuo JH, Anderson HU, Sparlin DM, Oxidation-reduction behavior of undoped and Sr-doped $LaMnO_3$: defect structure, electrical conductivity, and thermoelectric power, J. Solid State Chem. **87** (1990) 55–63. https://doi.org/10.1016/0022-4596(90)90064-5

80. Kamata H, Yonemura Y, Mizusaki J, Tagawa H, Naraya K, Sasamoto T, High temperature electrical properties of the perovskite-type oxide $La_{1-x}Sr_xMnO_{3-\delta}$, J. Phys. Chem. Solid. **56 (7)** (1995) 943–950. https://doi.org/10.1016/0022-3697(95)00019-4

81. Endo A, Fukunaga H, Wen C, Yamada K, Cathodic reaction mechanism of dense $La_{0.6}Sr_{0.4}CoO_3$ and $La_{0.81}Sr_{0.09}MnO_3$, Solid State Ionics, **135** (2000) 353–358. https://doi.org/10.1016/S0167-2738(00)00466-5

82. Mizusaki J, Saito T, Tagawa H, A chemical diffusion-controlled electrode reaction at the compact $La_{1-x}Sr_xMnO_3$/stabilized zirconia interface in oxygen atmospheres, J. Electrochem. Soc. **143 (10)** (1996) 3065–3073. https://doi.org/10.1149/1.1837165

83. Ioroi T, Hara T, Uchimoto Y, Ogumi Z, Takehara Z, Preparation of perovskite-type $La_{1-x}Sr_xMnO_3$ films by vapor-phase processes and their electrochemical properties, J. Electrochem. Soc. **145 (6)** (1998) 1999–2004. https://doi.org/10.1149/1.1838589

84. Mizusaki J, Tagawa H, Tsuneyoshi K, Sawata A, Reaction kinetics and microstructure of the solid oxide fuel cells air electrode $La_{0.6}Ca_{0.4}MnO_3$/YSZ, J. Electrochem. Soc. **138 (7)** (1991) 1867–1975. https://doi.org/10.1149/1.2085891

85. Ostergard MJL, Mogensen M. Ac impedance study of the oxygen reduction mechanism on $La_{1-x}Sr_xMnO_3$ in solid oxide fuel cells, Electrochim. Acta **38 (14)** (1993) 2015–2020. https://doi.org/10.1016/0013-4686(93)80334-V

86. van Heuveln FH, Bouwmeester HJM, Electrode properties of Sr-doped $LaMnO_3$ on yttria-stabilized zirconia. II. Electrode kinetics, J. Electrochem. Soc. **144 (1)** (1997) 134–140. https://doi.org/10.1149/1.1837375

87. Sasaki K, Wurth J-P, Gschwend R, Godickemeier M, Gauckler LJ, Microstructure-property relations of solid oxide fuel cell cathodes and current collectors, J. Electrochem. Soc. **143 (2)** (1996) 530–543. https://doi.org/10.1149/1.1836476

88. Takeda Y, Kanno R, Noda M, Tomida Y, Yamamoto O, Cathodic polarization phenomena of perovskite oxide electrodes with stabilized zirconia, J. Electrochem. Soc. **134 (11)** (1987) 2656–2661. https://doi.org/10.1149/1.2100267

89. Siebert E, Hammouche A, Kleitz M, Impedance spectroscopy analysis of $La_{1-x}Sr_xMnO_3$-yttria-stabilized zirconia electrode kinetics, Electrochim. Acta, **40 (11)** (1995) 1741–1753. https://doi.org/10.1016/0013-4686(94)00361-4

90. Adler SB, Lane JA, Steele BCH, Electrode Kinetics of Porous Mixed Conducting Oxygen Electrodes, J. Electrochem. Soc. **143 (11)** (1996) 3554–3564. https://doi.org/10.1149/1.1837252

91. Mitterdorfer A, Gauckler LJ, Identification of the reaction mechanism of the Pt, O_2(g)|yttria-stabilized zirconia system: Part I: General framework, modelling, and structural investigation, Solid State Ionics, **117** (1999) 187–202. https://doi.org/10.1016/S0167-2738(98)00341-5

92. Mitterdorfer A, Gauckler LJ, Identification of the reaction mechanism of the Pt, O_2(g)|yttria-stabilized zirconia system: Part II: Model implementation, parameter estimation, and validation, Solid State Ionics, **117** (1999) 203–217. https://doi.org/10.1016/S0167-2738(98)00340-3

93. Ni M, Leung MKH, Leung DYC, Micro-scale modelling of solid oxide fuel cells with micro-structurally graded electrodes, J. Power Sources, **168** (2007) 369–378. https://doi.org/10.1016/j.jpowsour.2007.03.005

94. Ananyev MV. Isotopic exchange of oxygen and hydrogen gas with oxide electrochemical materials [dissertation]. Yekaterinburg (Russia): Institute of high temperature electrochemistry; 2016. 391 p.

95. Gerischer H, Wechselstrompolarisation von Elektroden mit einem potentialbestimmenden Schritt beim Gleichgewichtspotential II, Z. Phys. Chem. **201** (1952) 55–67. https://doi.org/10.1515/zpch-1952-20105

96. Osinkin DA, Khodimchuk AV, Antonova EP, Bogdanovich NM, Understanding the oxygen reduction kinetics on $Sr_{2-x}Fe_{1.5}Mo_{0.5}O_{6-\delta}$: Influence of strontium deficiency and correlation with the oxygen isotopic exchange data, Solid State Ionics, **374** (2022) 115818. https://doi.org/10.1016/j.ssi.2021.115818

97. Almar L, Sz´asz J, Weber A, Ivers-Tiffee E, Oxygen Transport Kinetics of Mixed Ionic-Electronic Conductors by Coupling Focused Ion Beam Tomography and Electrochemical Impedance Spectroscopy, J. Electrochem. Soc. **164 (4)** (2017) F289–F297. https://doi.org/10.1149/2.0851704jes

98. Zupnik AE, Perfiliev MV, Karpachev SV, Polyarizaciay processa electrohimicheskogo vosstanovleniya pariv void v yacheykah s tverdim electrolitom [Polarization of electrochemical reduction of water vapor in cells with solid electrolyte], Electrohimiya, **7 (8)** (1971) 1163–1167.

99. Zupnik AE, Perfiliev MV, Karpachev SV, Impedance granicy razdela platinovih electrodov s tverdim electrolitom v atmosphere vodoroda I void [Impedance of the interface of platinum electrodes with solid electrolyte in hydrogen and water atmosphere], Electrohimiya, **7 (8)** (1971) 1188–1191.

100. Zupnik AE, Perfiliev MV, Karpachev SV, Impedance granicy platinoviy electrode / tverdiy electrolit v usloviyah katodnoy polyarizacii [Impedance of platinum electrode/solid electrolyte interface under cathodic polarization conditions], Electrohimiya, **8 (11)** (1972) 1639–1641.

101. Kuzin BL, Neuymin AD, Palguev SF, Anodnaya polarizaciya tonkih electrodov v kontakte s tverdim electrolitom v gazovoy srede H2+H2O perennogo sostava [Anodic polarization of thin nickel electrodes in contact with solid electrolyte in H2+H2O gas medium of variable composition], Electrohimiya, **9 (1)** (1973) 17–22.

102. Schouler EJL, Kleitz M, Forest E, Fernandez E, Fabry P, Overpotential of H_2-H_2O, Ni/YSZ electrodes in steam electrolyzers, Solid State Ionics, **5** (1981) 559–562. https://doi.org/10.1016/0167-2738(81)90316-7

103. Fernandez E. Electrolyse de la vapeur d'eau: characteristique de la reaction cathodique et conductivities de la zircone stabilisee [Ph.D. Theses]. Grenoble [France]; 1980. 105 p.

104. Kuzin BL. Investigation of electrode process kinetics on nickel electrode in contact with solid oxide electrolyte in H2+H2O atmosphere [dissertation]. Sverdlovsk [USSR]: Institute of electrochemistry; 1977. 156 p.

105. Mizusaki J, Tagawa H, Saito T, Kamitani K, et al., Hashimoto Preparation of nickel pattern electrodes on YSZ and their electrochemical properties in H_2-H_2O atmospheres, J. Electrochem. Soc. **141 (8)** (1994) 2129–2134. https://doi.org/10.1149/1.2055073

106. Nakagawa N, Sakurai H, Kondo K, Morimoto T, et al., Evaluation of the effective reaction zone at Ni(NiO)/zirconia anode by using an electrode with a novel structure, J. Electrochem. Soc. **142 (10)** (1995) 3474–3479. https://doi.org/10.1149/1.2050007

107. Holtappels P, Vinke IC, de Haart LGJ, Stimming U, Reaction of hydrogen/water mixtures on nickel-zirconia cermet electrodes. II. Ac polarization characteristics, J. Electrochem. Soc. **146 (8)** (1999) 2976–2982. https://doi.org/10.1149/1.1392038

108. de Boer B, Gonzalez M, Bowmeester HJM, Verweij H, The effect of the presence of fine YSZ particles on the performance of porous nickel electrodes, Solid State Ionics, **127** (2000) 269–276. https://doi.org/10.1016/S0167-2738(99)00299-4

109. Mogensen M, Skaarup S, Kinetic and geometric aspects of solid oxide fuel cell electrodes, Solid State Ionics, **86–88** (1996) 1151–1160. https://doi.org/10.1016/0167-2738(96)00280-9

110. Mogensen M, Lindegaard T. The kinetics of hydrogen oxidation on a Ni/YSZ SOFC electrode at 1000 °C. In: 3rd International Symposium on Solid Oxide Fuel Cells (SOFC-III); 1993; Honolulu, HI, USA. 484–493.

111. de Boer B. SOFC Anode: hydrogen oxidation at porous nickel and nickel/yttria-stabilised zirconia cermet electrodes [Ph.D. thesis]. Enschede (Netherlands): University of Twente; 1998. 161 p.

112. Lee WY, Wee D, Ghoniem AF, An improved one-dimensional membrane electrode assembly model to predict the performance of solid oxide fuel cell including the limiting current density, J. Power Sources, **186** (2009) 417–427. https://doi.org/10.1016/j.jpowsour.2008.10.009

113. Jiang SP, Badwal SPS, An electrode kinetics study of H2 oxidation on Ni/Y_2O_3-ZrO_2 cermet electrode of the solid oxide fuel cell, Solid State Ionics, **123** (1999) 209–224. https://doi.org/10.1016/S0167-2738(99)00124-1

114. Jiang SP, Badwal SPS, Hydrogen oxidation at the nickel and platinum electrodes on yttria-tetragonal zirconia electrolyte, J. Electrochem. Soc. **144 (11)** (1997) 3777–3784. https://doi.org/10.1149/1.1838091

115. Bieberle A, Meier LP, Gauckler LJ, The electrochemistry of Ni pattern anodes used as solid oxide fuel cell model electrodes, J. Electrochem. Soc. **148 (6)** (2001) A646–A656. https://doi.org/10.1149/1.1372219

116. Bieberle A. The electrochemistry of solid oxide fuel cell anodes: experiments, modeling, and simulation [Ph.D. thesis]. Zurich (Switzerland): Swiss Federal Institute of Technology; 2000. 222 p.

117. Bieberle A, Gauckler LJ, State-space modeling of the anodic SOFC system Ni, H_2-H_2O/YSZ, Solid State Ionics, **146** (2002) 23–41. https://doi.org/10.1016/S0167-2738(01)01004-9

118. Bessler WG, Warnatz J, Goodwin DG, The influence of equilibrium potential on the hydrogen oxidation kinetics of SOFC anodes, Solid State Ionics, **177** (2007) 3371–3383. https://doi.org/10.1016/j.ssi.2006.10.020

119. Jiang Y, Virkar AV, Fuel composition and diluent effects on gas transport and performance of anode-supported SOFCs, J. Electrochem. Soc. **150 (7)** (2003) A942–A951. https://doi.org/10.1149/1.1579480

120. Matsuzaki Y, Yasuda I, Electrochemical oxidation of H_2 and CO in a H_2-H_2O-CO-CO_2 system at the interface of a Ni-YSZ cermet electrode and YSZ electrolyte, J. Electrochem. Soc. **147 (5)** (2000) 1630–1635. https://doi.org/10.1149/1.1393409

121. Eguchi K, Kojo H, Takeguchi T, Kikuchi R, et al., Fuel flexibility in power generation by solid oxide fuel cells, Solid State Ionics, **152–153** (2002) 411–416. https://doi.org/10.1016/S0167-2738(02)00351-X

122. Sasaki K, Hori Y, Kikuchi R, Eguchi K, et al., Uchida Current-voltage characteristics and impedance analysis of solid oxide fuel cells for mixed H2 and CO gases, J. Electrochem. Soc. **149 (3)** (2002) A227–A233. https://doi.org/10.1149/1.1435357

123. Etsell TH, Flengas SN, Overpotential behavior of stabilized zirconia solid electrolyte fuel cells, J. Electrochem. Soc. **118 (12)** (1971) 1890–1900. https://doi.org/10.1149/1.2407862

124. Lauvstad GO, Tunold R, Sunde S, Electrochemical oxidation of CO on Pt and Ni point electrodes in contact at

yttria-stabilized zirconia electrolyte, J. Electrochem. Soc. **149 (12)** (2002) E497–E505. https://doi.org/10.1149/1.1518484

125. Somov SI, Perfiliev MV, Polyarizacionnye harakteristiki electrodnoy sistemy $CO + CO_2/M + CeO_{2-x}/0.91ZrO_2 + 0.09Y_2O_3$ [Polarization characteristics of the electrode system $CO + CO_2/M + CeO_{2-x}/0.91ZrO_2 + 0.09Y_2O_3$. In: Electrodnye reakcii v tverdyh electrolitah; 1990; Sverdlovsk, 80–90.

126. Zhu T, Fowler DE, Poeppelmeier KR, Han M, Barnett SA, Hydrogen Oxidation Mechanisms on Perovskite Solid Oxide Fuel Cell Anodes, J. Electrochem. Soc. **163 (8)** (2016) F952–F961. https://doi.org/10.1149/2.1321608jes

127. Chen M, Chen D, Chang M, Hu H, Xu Q, New Insight into Hydrogen Oxidation Reaction on $La_{0.3}Sr_{0.7}Fe_{0.7}Cr_{0.3}O_{3-\delta}$ Perovskite as a Solid Oxide Fuel Cell Anode, J. Electrochem. Soc. **164** (2017) F405–F411. https://doi.org/10.1149/2.1571704jes

128. Niu B, Jin F, Yang X, Feng T, He T, Resisting coking and sulfur poisoning of double perovskite $Sr_2TiFe_{0.5}Mo_{0.5}O_{6-\delta}$ anode material for solid oxide fuel cells, Int. J. Hydrogen Energy, **43 (6)** (2018) 3280–3290. https://doi.org/10.1016/j.ijhydene.2017.12.134

129. Bian L, Duan C, Wang L, Zhu L, et al., Electrochemical performance and stability of $La_{0.5}Sr_{0.5}Fe_{0.9}Nb_{0.1}O_{3-\delta}$ symmetric electrode for solid oxide fuel cells, J. Power Sources, **399** (2018) 398–405. https://doi.org/10.1016/j.jpowsour.2018.07.119

130. Niu B, Jin F, Fu R, Feng T, Shen Y, Liu J, He T, Pd-impregnated $Sr_{1.9}VMoO_{6-\delta}$ double perovskite as an efficient and stable anode for solid-oxide fuel cells operating on sulfur-containing syngas, Electrochim. Acta, **274** (2018) 91–102. https://doi.org/10.1016/j.electacta.2018.04.066

131. Ammal SC, Heyden A, Reaction kinetics of the electrochemical oxidationof CO and syngas fuels on a $Sr_2Fe_{1.5}Mo_{0.5}O_{6-\delta}$ perovskite anode, J. Mater. Chem. A, **3** (2015) 21618–21629. https://doi.org/10.1039/C5TA05056A

132. Yang Y, Li Y, Jiang Y, Zheng M, et al., The electrochemical performance and CO_2 reduction mechanism on strontium doped lanthanum ferrite fuel electrode in solid oxide electrolysis cell, Electrochim. Acta, **284** (2018) 159–167. https://doi.org/10.1016/j.electacta.2018.07.187

133. Li J, Wei B, Wang C, Zhou Z, Lu Z, High-performance and stable $La_{0.8}Sr_{0.2}Fe_{0.9}Nb_{0.1}O_{3-\delta}$ anode for direct carbon solid oxide fuel cells fueled by activated carbon and corn straw derived carbon, Int. J. Hydrogen Energy, **43 (27)** (2018) 12358–12367. https://doi.org/10.1016/j.ijhydene.2018.04.176

134. Osinkin DA, Kinetics of CO oxidation and redox cycling of $Sr_2Fe_{1.5}Mo_{0.5}O_{6-\delta}$ electrode for symmetrical solid state electrochemical devices, J. Power Sources, **418** (2019) 17–23. https://doi.org/10.1016/j.jpowsour.2019.02.026